J. Membrane Biol. 106, 13–28 (1988)

The Journal of
Membrane Biology

Voltage Dependence of Cellular Current and Conductances in Frog Skin

W. Nagel,† J.F. García-Díaz,‡ and A. Essig‡

‡Department of Physiology, Boston University School of Medicine, Boston, Massachusetts 02118 and †Department of Physiology, University of Munich, D-8000 Munich 2, Federal Republic of Germany

Summary. Knowledge of the voltage dependencies of apical and basolateral conductances is important in determining the factors that regulate transcellular transport. To gain this knowledge it is necessary to distinguish between cellular and paracellular currents and conductances. This is generally done by sequentially measuring transepithelial current/voltage (I_t/V_t) and conductance/voltage (g_t/V_t) relationships before and after the abolition of cellular sodium transport with amiloride. Often, however, there are variable time-dependent and voltage-dependent responses to voltage perturbation both in the absence and presence of amiloride, pointing to effects on the paracellular pathway. We have here investigated these phenomena systematically and found that the difficulties were significantly lessened by the use of an intermittent technique, measuring I_t and g_t before and after brief (<10 sec) exposure to amiloride at each setting of V_t. I/V relationships were characterized by these means in frog skins (*Rana pipiens*, Northern variety, and *Rana temporaria*). Cellular current, I_c, decreased with hyperpolarization (larger serosa positive clamps) of V_t. Derived I_c/V_t relationships between $V_t = 0$ and 175 mV (serosa positive) were slightly concave upwards. Because values of cell conductance, g_c, remained finite, it was possible to demonstrate reversal of I_c. Values of the reversal potential V^r averaged 156 ± 14 (SD, $n = 18$) mV. Simultaneous microelectrode measurements permitted also the calculation of apical and basolateral conductances, g_a and g_b. The apical conductance decreased monotonically with increasing positivity of V_t (and V_a). In contrast, in the range in which the basolateral conductance could be evaluated adequately ($V_t < 125$ mV), g_b increased with more positive values of V_t (and V_b). That is, there was an inverse relation between g_b and cellular current at the quasi-steady state, 10–30 sec after the transepithelial voltage step.

Key Words cell potential · amiloride · sodium transport · reversal potential

Introduction

It has been proposed that an increase in the rate of apical sodium entry in epithelia leads, by a still unknown mechanism, to a parallel increase in basolateral conductance that would serve both to facilitate continuing transcellular transport and to protect intracellular ionic composition [20]. Since change in apical Na entry brings about change in cell potential, it is possible that the observed effects on basolateral conductance can be a consequence of its voltage dependency. In this study we analyze the responses of apical and basolateral conductances of frog skin to changes in the corresponding membrane voltages, elicited by clamping the transepithelial potential to values between −50 and 200 mV (serosa positive). Since the voltage-induced changes in cell conductances in frog skin have a half time of several seconds [13], we measured currents and cell voltage 10–30 sec after changing the transepithelial voltage. To determine cell conductances, transepithelial conductance and fractional apical resistance were measured, at the same time, from the deflections in current and apical voltage induced by short, 10-mV pulses superimposed on the holding transepithelial voltage.

In order to characterize cellular conductances it was necessary, of course, to differentiate between cellular and paracellular currents[1]. One technique often applied to this problem is the sequential determination of current/voltage (I/V) relationships, first under control conditions and then following abolition of transcellular transport by amiloride [1, 18, 21, 23]. However, as previously reported [4, 15], exposure to amiloride importantly affects paracellular conductance (particularly in the presence of apical Cl solutions), complicating the interpretation of I/V relationships. We have characterized further the problems encountered using amiloride and found that, with the use of substitutes for apical Cl

[1] For simplicity, we shall use the term "cellular" to refer to transport via principal cells and "paracellular" to refer to transport by way of extracellular and/or mitochondria-rich cells.

and brief intermittent exposure to amiloride at each setting of V_t, it was possible to minimize changes of paracellular conductance. This allowed us to characterize the response of cellular conductance to change in voltage. Considering also measurements of intracellular potentials, it was then possible to characterize the quasi-steady-state voltage dependencies of the apical and basolateral conductances.

Materials and Methods

The experiments were performed on abdominal skins of frogs (*Rana temporaria* or the Northern variety of *Rana pipiens*). The animals were maintained in flowing tap water either at low temperature (4°C) or at room temperature (23°C). After sacrifice, the skin was mounted, apical side up, in a modified Ussing type chamber, which was open at the top for microelectrode access [14]. Both surfaces were continuously perfused with Ringer solution. The serosal solution was NaCl Ringer (composition in mM: 110 Na; 2.5 K; 1 Ca; 112 Cl; 3.5 HEPES; pH 8.0). The mucosal fluid was either NaCl Ringer or Ringer in which 110 mM NaCl was replaced by the Na salt of nitrate or gluconate. The latter solutions were employed if the tissues had excessive conductance which disappeared after replacement of mucosal chloride or addition of amiloride [4, 14]. (We made no adjustments for the lowering of calcium activity in gluconate because we have noted no change in short-circuit current and membrane conductance even on lowering calcium to trace levels.) The perfusion rate was 2–5 ml/min on the serosal side and 5–10 ml/min on the mucosal side, with each chamber volume approximately 0.3 ml. Change of the mucosal perfusion solution was made using a magnetic valve with minimal dead space (#330-12L3, Angar Scientific, New Brunswick, NJ) and was virtually complete within 5 sec. Amiloride was applied at the mucosal surface at a concentration of 10 to 50 μM.

The tissues were voltage clamped to desired transepithelial potentials using an automatic clamping/microelectrode amplifier system (Biomedizinische Instrumente, Germering, FRG). This device permits measurement of the current (I_t) and the potential difference across the epithelium (V_t) and across the outer (apical) border (V_a), as well as the continuous on-line determination of the tissue conductance (g_t) and apical fractional resistance (voltage-divider ratio) (f_a). This is accomplished by the use of appropriately triggered sample-and-hold circuitry and by applying 10-mV V_t pulses every 1–2 sec, lasting 150–180 msec, occasionally up to 400 msec [25]. V_a was observed on a storage oscilloscope (Tektronix 5101A) to ensure that capacitative transients were completely dissipated prior to sampling [5, 18]. Data were recorded on a multichannel strip chart recorder (Servogor 460, BBC-Metrawatt, Nurenberg, FRG) with 250-mm chart width and automatic bucking of the zero point for I_t. This permitted reading I_t with an accuracy of 0.5 μA/cm^2 even at levels of 200–300 μA/cm^2; g_t was read to 0.5% of the full scale setting (0.5 to 2 mS/cm^2) and V_a and f_a were read to 1 mV and 0.01, respectively.

Microelectrodes for determination of intracellular potentials were prepared from Omega-dot fiber capillaries (F. Haer, Ann Arbor, MI) on a horizontal microelectrode puller (Model M1, Industrial Science Assoc., Flushing, NY, or Brown-Flaming P77, Sutton Instr., San Rafael, CA) and had input resistances of 40–60 MΩ after filling with 1.5 M KCl. They were advanced across the apical border into individual cells of the epithelium with the aid of a stepping motor micromanipulator (MF500, Biomedizinische Instrumente, Germering, FRG). Criteria for acceptable intracellular recordings have been described previously [4, 11].

During the course of the study two different voltage-clamping protocols were developed for the analysis of the components of the current and conductance. In one series (referred to as "sequential technique"), V_t was sequentially clamped to increasing values up to 200 mV (serosa positive), e.g., 0, 50, 100, 150, 200 mV; sometimes values between 0 and −50 mV were included. The duration of each clamp was between 10 and 30 sec and was identical throughout a particular experiment. Note that at each setting of these holding values of V_t, the 10-mV rapid pulses were continuously applied to determine transepithelial conductance and apical fractional resistance. After completion of the initial clamp sequence, amiloride was added, and following depression of the short-circuit current to less than 5% of the initial level, which took between 2 and 5 min, a similar sequence was used to characterize the behavior of the amiloride-insensitive pathway and, by difference, that of the amiloride-sensitive pathway. It was often observed that the conductance both with and without amiloride changed considerably and rapidly during the periods of voltage perturbation (*see below*). Furthermore, it appeared that the temporal evolution of the conductance differed in the presence and absence of transcellular sodium flow. These effects were larger and more frequent in the presence of apical chloride.

Hence we modified the technique in an attempt to eliminate uncertainty regarding the temporal behavior of the shunt. In this series (referred to as "intermittent technique"), following equilibration at short circuit, the tissues were voltage clamped to a value between 0 and 200 mV. After stabilization of the electrical characteristics, which required between 10 and 20 sec, amiloride was perfused at a high rate and the changes of the electrical parameters induced within the next 5–10 sec were observed. The tissue was then again short circuited and amiloride was washed away. When the initial steady-state conditions were restored, V_t was clamped to a new level and the above procedure was repeated. Four to six such determinations were used to construct the relationships between the transepithelial and apical potential differences and the amiloride-sensitive current and conductances. Particular emphasis was placed on settings of V_t above the reversal point of the amiloride-inhibitable current (*see below*).

The following abbreviations were employed:

f_a fractional apical resistance, evaluated from $\delta V_a/\delta V_t$

g conductance (mS)

I current (μA; positive from apical to basolateral surface)

V potential difference (mV); reference: mucosal solution

δ refers to changes induced by the 10-mV V_t pulses of 180–400 msec duration.

Δ refers to changes induced by the application of amiloride.

Subscripts: a, b, c, j, l, p, and t indicate the apical, basolateral, cellular, junctional, lateral space, paracellular and transepithelial variable, respectively.

Superscripts: o indicates measurement at short circuit; r refers to the voltage at the point of cellular current reversal; $'$ indicates measurement in the presence of amiloride.

All currents and conductances are normalized for 1 cm^2 tissue area.

Average values are given as mean ± SD.

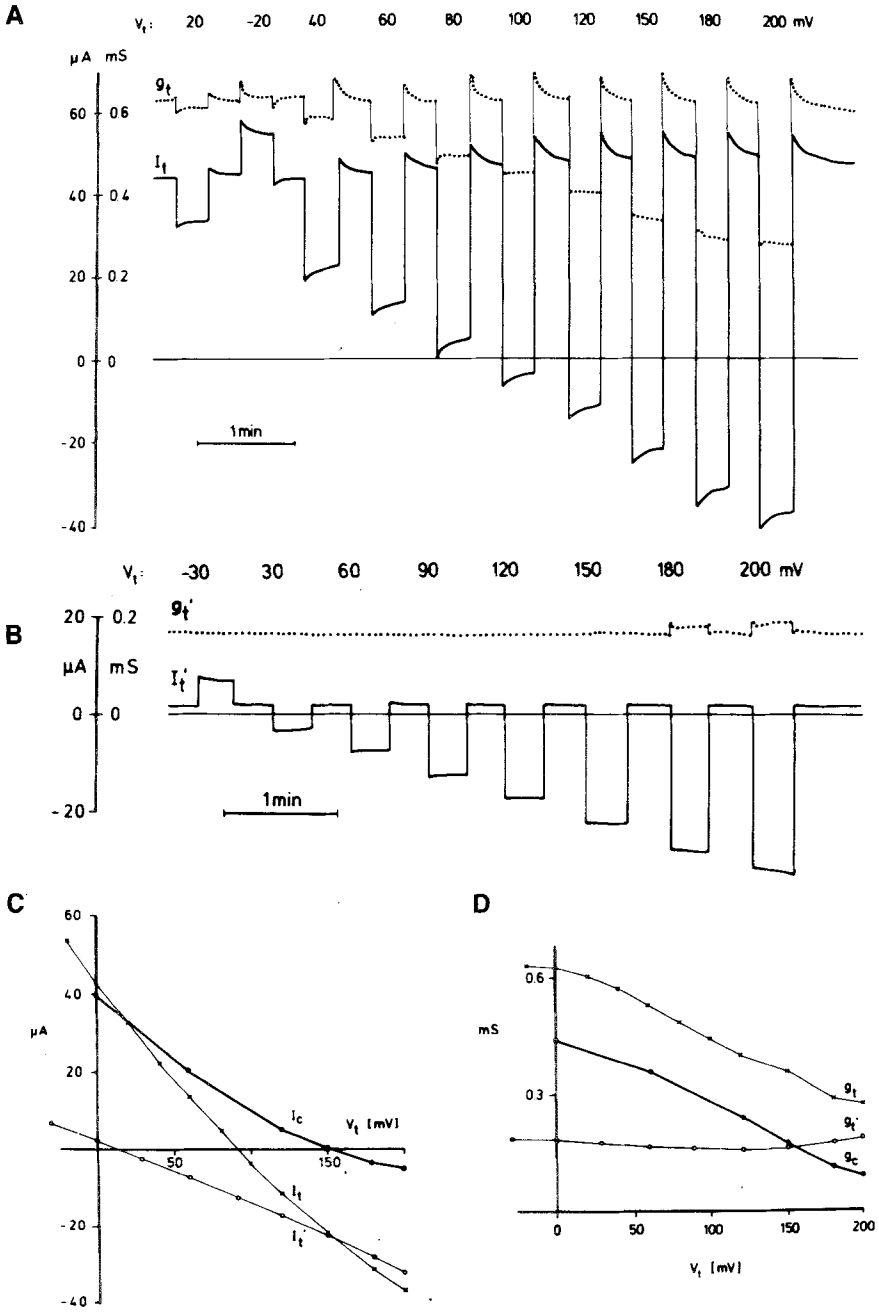

Fig. 1. Response of transepithelial current I_t and conductance g_t to clamping of V_t to different levels in the absence (*A*) and presence (*B*) of 50 μM amiloride, and the associated current-voltage (*C*) and conductance-voltage (*D*) relationships. The deflections in I_t induced by the 10-mV pulses (used to measured g_t) are not shown, since the I_t output was taken from the sample-and-hold circuit. Note that following each voltage step V_t is returned to 0 mV. I_t and I_t' are the currents in the absence and presence of amiloride respectively, and $I_c = I_t - I_t'$; equivalent notation is employed for the conductances. The apical solution was nitrate Ringer

Results

Transepithelial Analysis; Sequential Technique

Figure 1 shows the voltage dependence of the current and conductance of an exceptionally stable tissue, studied in mucosal nitrate Ringer solution. Observations were made first in the absence of amiloride (Fig. 1*A*) and then in its presence (Fig. 1*B*). Positive V_t clamps induced prompt decrease of g_t to a near-constant value, with relaxation to the original level on return to the short-circuit state (Fig. 1*A*). The amiloride-insensitive conductance g_t' was unaffected by the voltage steps, except for a slight increase at the highest values of V_t (Fig. 1*B*), so that the amiloride-sensitive currents and conductances could be unambiguously calculated as the difference of values in the absence and presence of amiloride (Fig. 1*C* and *D*). The apparent cellular current I_c became zero at $V_t = 150$ mV. Note that I_c

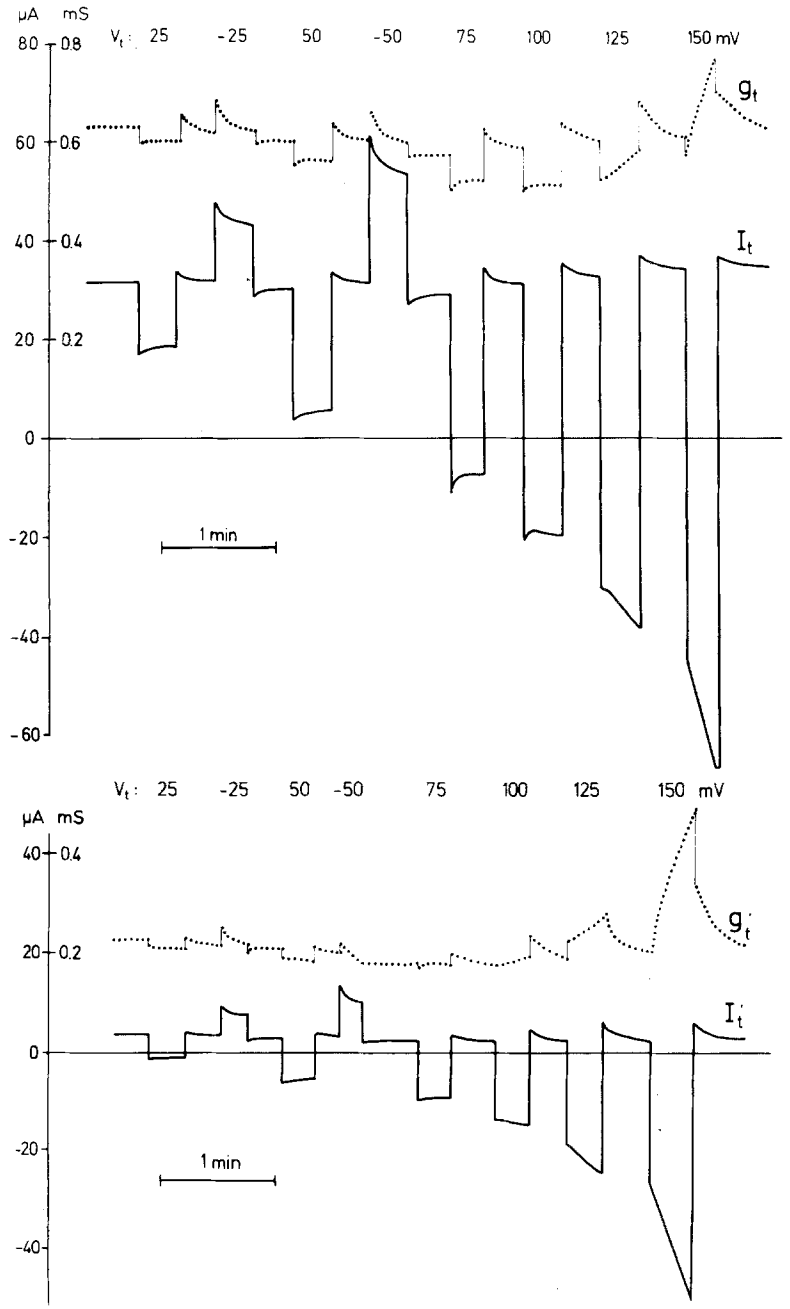

Fig. 2. Response of transepithelial current and conductance to V_t clamp steps in the absence (upper panel) and presence (lower panel) of 50 μM amiloride. *See* text and Fig. 1 legend for further explanations. The apical solution was chloride Ringer

was reversed at the highest levels of V_t (Fig. 1*C*). We consider this a necessary criterion for reliable determination of the reversal potential, because mere decrease of I_c to near zero might result from either abolition of the net driving force or diminution of the cellular conductance.

With the regularity observed in the above described study, it was straightforward to evaluate cellular parameters. Although similarly stable responses were found in other experiments (more frequently in the absence than in the presence of mucosal chloride), these were the exception. More typical findings are shown in Fig. 2, representing a study in the presence of mucosal chloride. The characteristic response of g_t to hyperpolarization in the absence of amiloride (upper trace) was again an instantaneous decrease, but at the higher levels of V_t (>100 mV) this was followed promptly by a progressive increase. At V_t = 150 mV, the secondary change in g_t was so large and rapid that the initial decrease was almost undetectable. The lower trace shows that sustained voltage steps affected g_t' nearly identically, suggesting that the secondary effects were due to alterations of paracellular conduc-

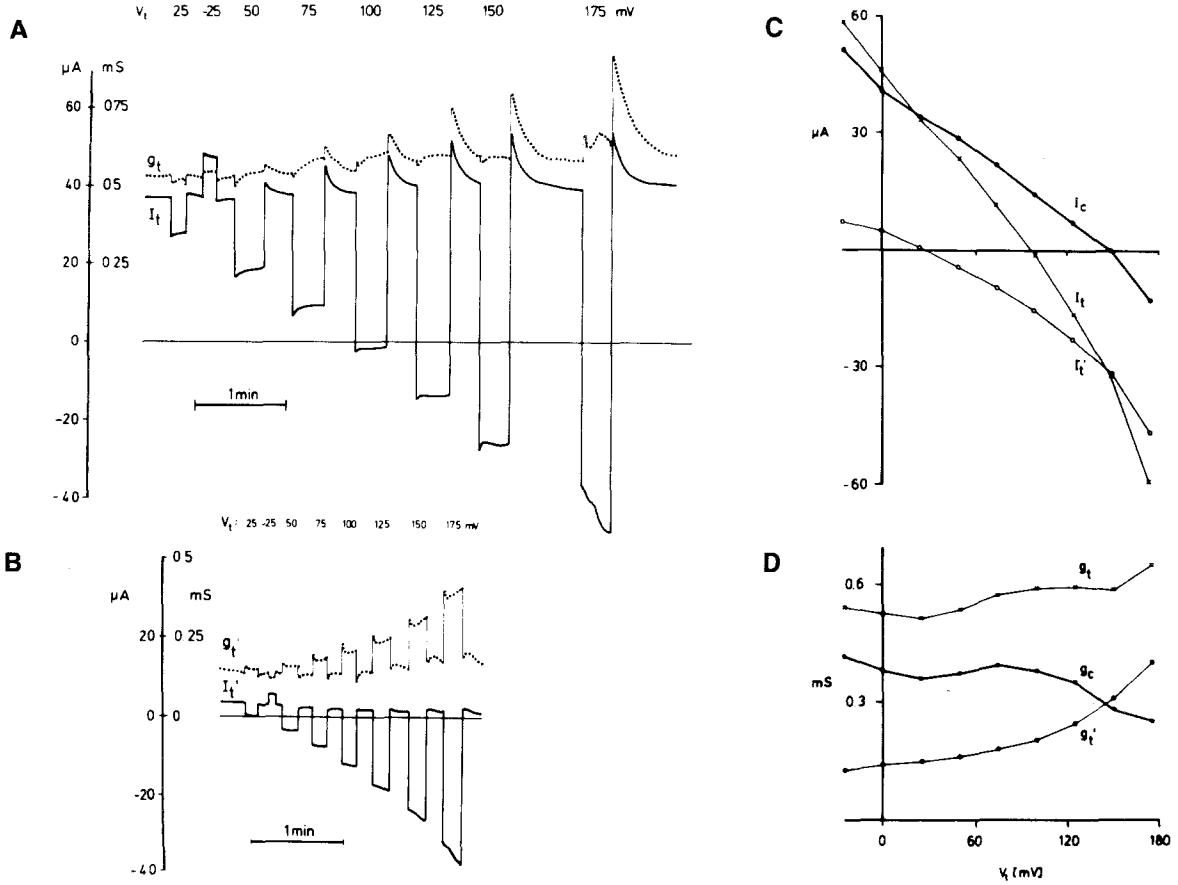

Fig. 3. Response of I_t and g_t to perturbations of V_t in the absence (*A*) and presence (*B*) of 50 μM amiloride, and the associated current-voltage (*C*) and conductance-voltage (*D*) relationships determined from measurements 10 sec after the onset of the voltage-clamp steps. I_c reversed at V_t = 150 mV. The apical solution was nitrate Ringer

tance. In addition, in this experiment, amiloride induced a progressive decrease of conductance (not shown in the figure), which was uncorrelated with the decrease of short-circuit current. Hence the paracellular pathway was in different states before and after amiloride. This has been described previously [14]. Even larger side effects were observed in tissues with higher spontaneous conductance. Replacement of mucosal chloride did not then eliminate the extreme time and voltage-dependent changes of conductance. Under these circumstances, it is evidently not possible to deduce meaningful I_c/V_t and g_c/V_t relationships.

Accordingly, attention was directed at tissues with lower conductance in an attempt to learn whether precise timing would permit characterization of the influence of voltage on cell parameters. Figure 3 shows an experiment in which nitrate replaced mucosal chloride. Both in the absence (Fig. 3*A*) and in the presence (Fig. 3*B*) of 50 μM amiloride, substantial time and voltage-dependent changes of g_t can be seen. These are particularly evident during the relaxation periods at short circuit in the unblocked state, and at the higher levels of V_t in the presence of amiloride. It should be noted that g_t' had already increased at the time of its first determination after the voltage step, i.e., within less than 1 sec.[2] Using the values of current and conductance measured 10 sec after perturbation of V_t gave the relationships presented in Figs. 3*C* and *D*. It will be shown below that this type of voltage dependence of cellular current and conductance is plausible, but the uncertainty of analysis under these circumstances is evident.

Figure 4 shows results of 23 experiments employing the sequential technique in which g_c was taken as the difference between g_t and g_t', each measured within 20 sec after the onset of the volt-

[2] For higher temporal resolution, we have performed some experiments shortening the 10-mV pulse to 50–80 msec and increasing its frequency up to 10 Hz. These experiments showed that g_t and g_t' had often increased considerably as early as 100–150 msec after the voltage step.

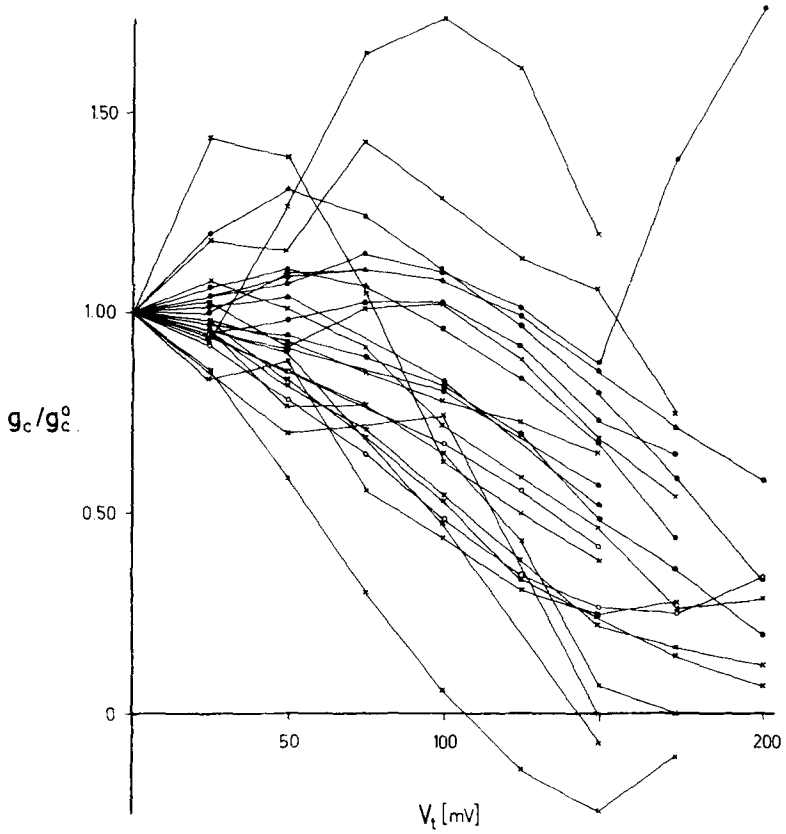

Fig. 4. Voltage dependence of g_c obtained with the sequential technique. Each value of g_c at a given setting of V_t was normalized by expressing it as a fraction of the value g_c^0 at short-circuit in the same tissue. Crosses, filled and open circles represent apical chloride, nitrate and gluconate, respectively

age step. In general, g_c appeared to decrease with increasing V_t; however, there was deviation from this pattern in several cases. In 18 instances, reversal of I_c was observed between 70 and 180 mV (average: 136 ± 8 mV). In five cases, V^r was undefined, i.e., there was no intercept of $I_t - I_t'$ on the voltage axis.

Transepithelial Analysis; Intermittent Technique

The above findings demonstrate that in favorable cases the sequential technique delineates fairly consistent response to voltage-clamp steps. Nevertheless, systematic analysis of cellular behavior becomes somewhat arbitrary in the face of poorly defined time and voltage dependencies. We attempted, therefore, to improve accuracy by the use of an alternative protocol in which at each level of V_t tissues were exposed only briefly to amiloride (*see* Materials and Methods).

The results of a representative study are shown in Fig. 5. As is seen from the reproduction of the original record (insets), temporal effects were small, and the magnitudes of the amiloride-sensitive currents and conductances were well defined. It is to be noted that although amiloride regularly depressed tissue conductance, at V_t = 190 and 200 mV it *increased* transepithelial current, indicating inhibition of reverse cellular current. Presuming independence of cellular and paracellular function, the voltage dependencies of I_c and g_c deduced from this record are as shown in the figure. Since it was possible to demonstrate reversal of I_c, its intercept gives a meaningful value of the reversal potential V^r.

Figure 6 demonstrates the general finding that both the composition of the mucosal solution and the protocol influence the apparent voltage dependence of currents and the quantification of V^r. The plots show that with both chloride and nitrate Ringer solutions the sequential technique underestimated V^r, as judged by the values derived with the intermittent technique (arrows). With chloride, however, the discrepancy was great, whereas with nitrate the two values were close. These findings indicate that the intermittent technique is more reliable than the sequential technique, particularly in the presence of mucosal chloride. It should be noted, however, that the intermittent administration and removal of amiloride is time consuming, so that the technique can be used only on temporally stable tissues. The results of experiments used to evaluate I_c are summarized in Fig. 7. In every case presented here, g_c remained finite at values of V_t =

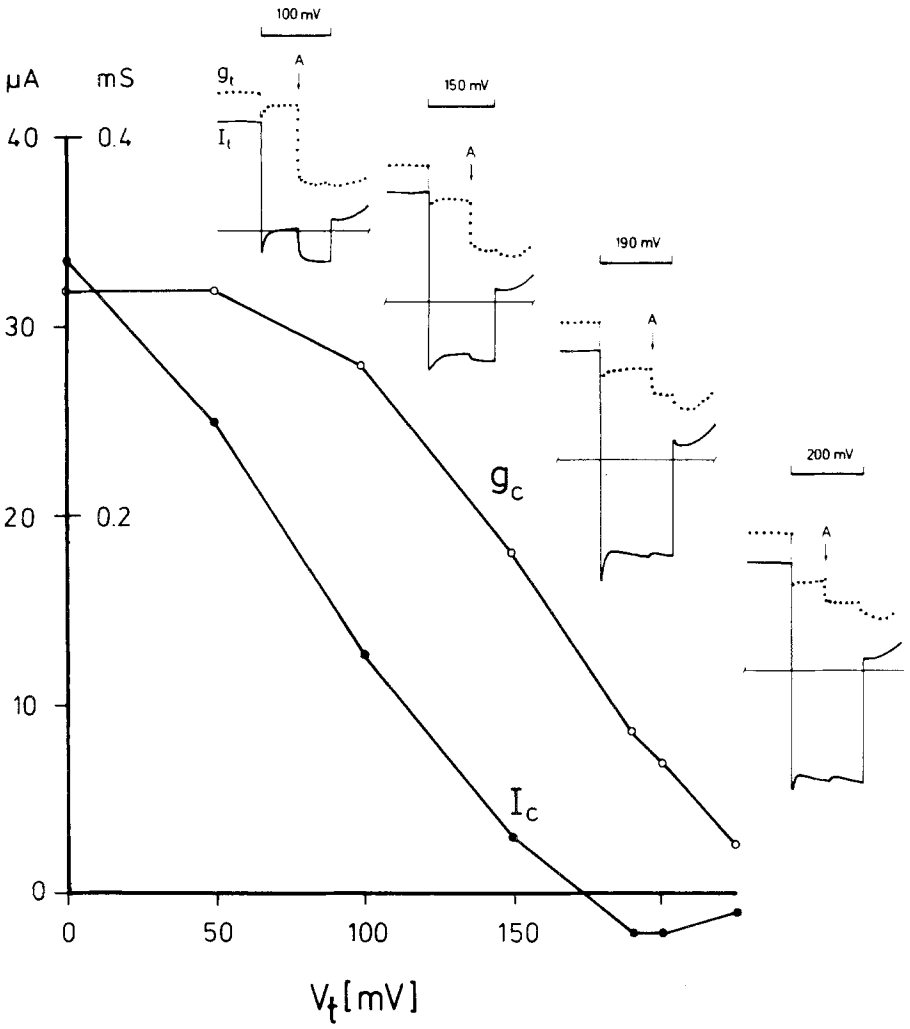

Fig. 5. Demonstration of intermittent technique: response of I_t and g_t to 20 μM amiloride at various settings of V_t (insets), and voltage dependence of I_c and g_c. Each voltage step lasted for 30 sec. Addition of amiloride is indicated by the vertical arrows marked *A*

V^r.[3] I_c decreased monotonically with increasing V_t, and in every case reversal of I_c was observed. V^r ranged from 139 to 185 mV, averaging 156 ± 14 mV. In contrast to the behavior of I_c, the dependence of g_c on V_t was complex (Fig. 8). The intracellular measurements presented below indicate that this behavior is due to the opposite voltage dependencies of apical and basolateral conductances.

Microelectrode Measurements

In experiments that employed the "intermittent technique," microelectrode measurements of intracellular potentials and cell membrane resistance ra-

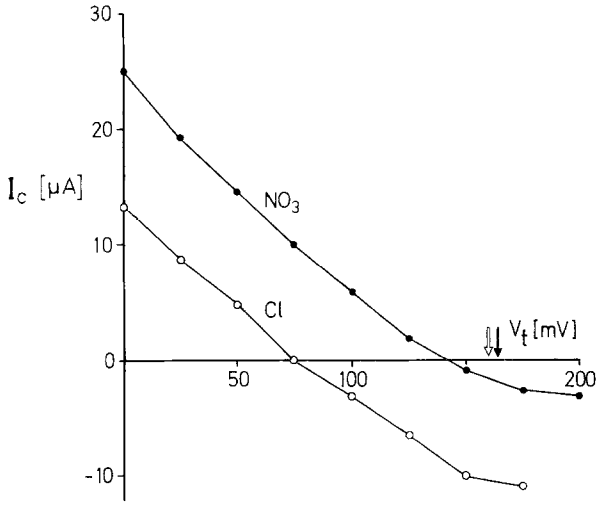

Fig. 6. Influence of apical anion composition and protocol on the apparent voltage dependence of I_c. The lines were derived by use of the sequential technique; the arrows indicate values of V^r obtained with the intermittent technique. Filled and open symbols represent mucosal nitrate and chloride, respectively

[3] Occasionally it was observed that g_c decreased to values near zero at $V_t < V^r$, particularly if gluconate or methylsulfate replaced mucosal chloride. Since reliable estimates of V^r cannot be obtained under such conditions, these cases were not included in our analysis.

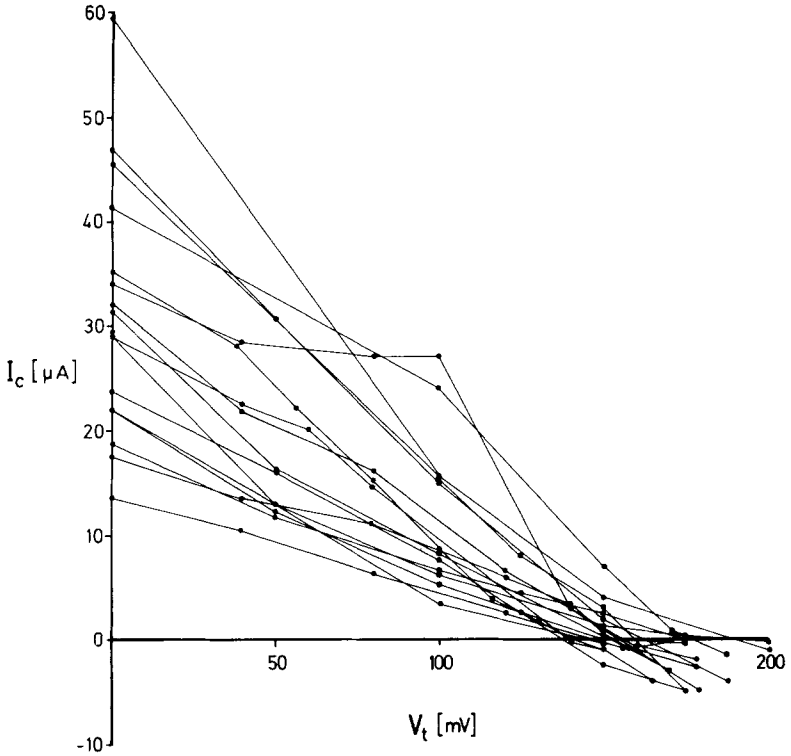

Fig. 7. Voltage (V_t) dependence of I_c for experiments employing the intermittent technique

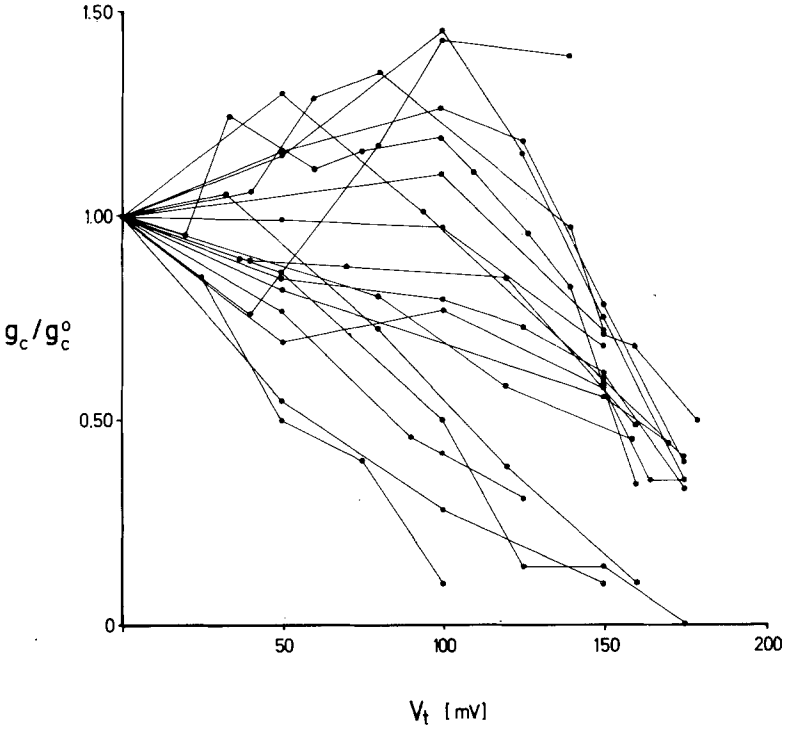

Fig. 8. Voltage (V_t) dependence of g_c, obtained with intermittent exposure to amiloride. (*Compare* Fig. 4.) g_c values are normalized as explained in the legend to Fig. 4.

tios were carried out. Representative results of one such experiment are shown in Figs. 9 and 10. The upper panel of Fig. 9*A* depicts the behavior of V_a and f_a on clamping V_t at six levels between 0 and 175 mV, followed by the rapid application of amiloride at each level. The initial values of V_a and f_a at short circuit are low, as occasionally seen in frog skin. After addition of amiloride, they increase to

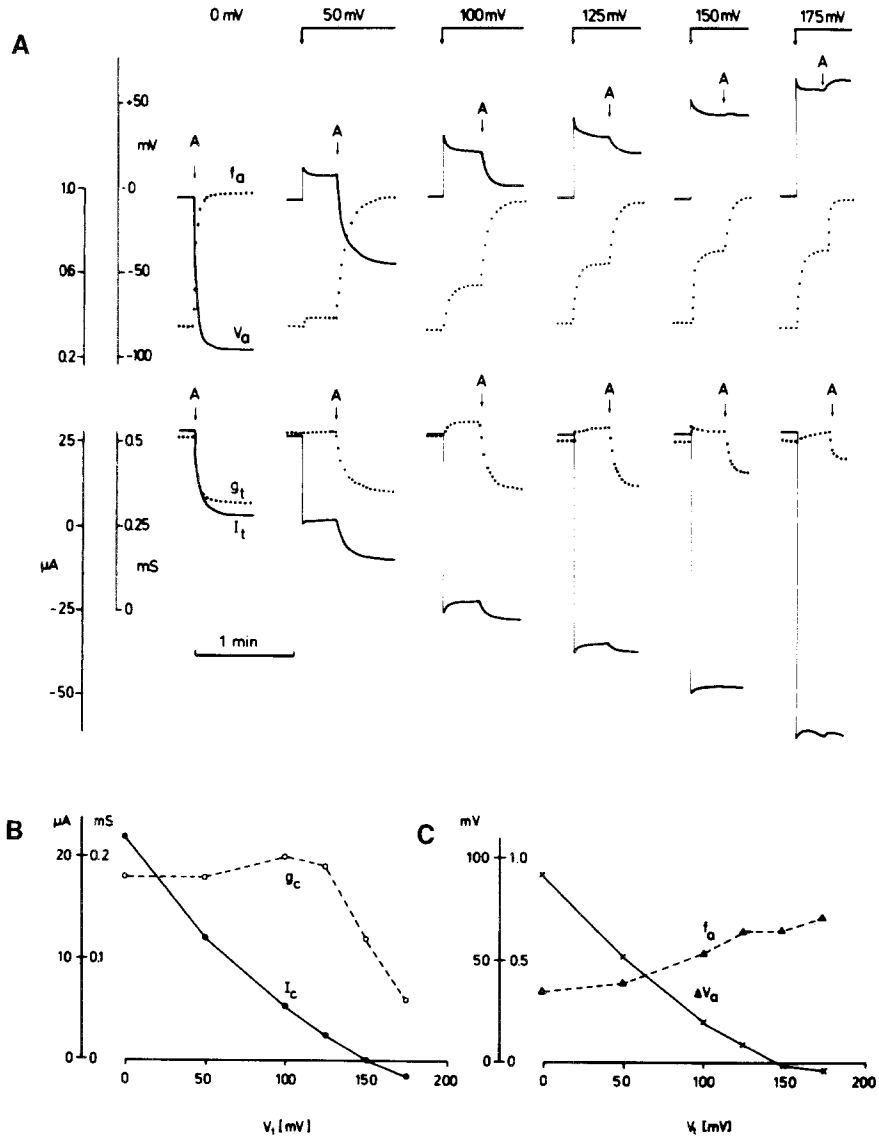

Fig. 9. Combined analysis of epithelial and cellular parameters (intermittent technique). (*A*) Response of apical voltage V_a and voltage-divider ratio f_a, and transepithelial current I_t and conductance g_t to 50 μM amiloride at various levels of V_t. V_t, initially 0 mV, was stepped to the stated value at the time indicated by the beginning of the bar. Amiloride was added when indicated by the arrows marked *A*. The change in V_a following amiloride defines ΔV_a. (*B*) Voltage (V_t) dependence of I_c and g_c. (*C*) Voltage dependence of ΔV_a and f_a

−95 mV and near 1.0, respectively. With increase of V_t, the change in V_a (ΔV_a) induced by amiloride became smaller (*see also* Fig. 9*C*). Fortuitously, V_t was set to the value of the reversal potential V^r on clamping to 150 mV, so that amiloride then had essentially no effect on V_a. At V_t = 175 mV, V_a became more positive following amiloride, consistent with the abolition of reverse current. The lower panel of Fig. 9*A* shows the corresponding responses of I_t and g_t. Addition of amiloride at V_t = 150 mV had no effect on I_t, confirming the inference from the microelectrode data that this potential represents V^r, at which the cellular current is zero (*see also* Fig. 9*B*).

Figure 9*B* and *C* show the voltage dependence of cellular parameters determined from the data of Fig. 9*A*. Increasing V_t reduced both I_c and the change in apical voltage V_a induced by amiloride, ΔV_a. In all experiments ΔV_a was roughly proportional to the magnitude of I_c; indeed, values of V^r obtained by interpolation of ΔV_a to the point of polarity reversal were nearly identical to those deduced from the corresponding interpolation of I_c. In 18 experiments, the mean value of V_a at the reversal potential was 47 ± 14 mV.

Fractional apical resistance, f_a, increased progressively with V_t as shown in Fig. 9*C*. From the values of f_a and g_c (Fig. 9*B*) it is possible to calculate the apical and basolateral conductances (g_a and g_b) at each setting of V_t. Because in this experiment f_a with amiloride was near 1.0 for all the values of V_t, the conductances were calculated according to the standard formulation (Appendix, Model A), which assumes discrete cellular and paracellular

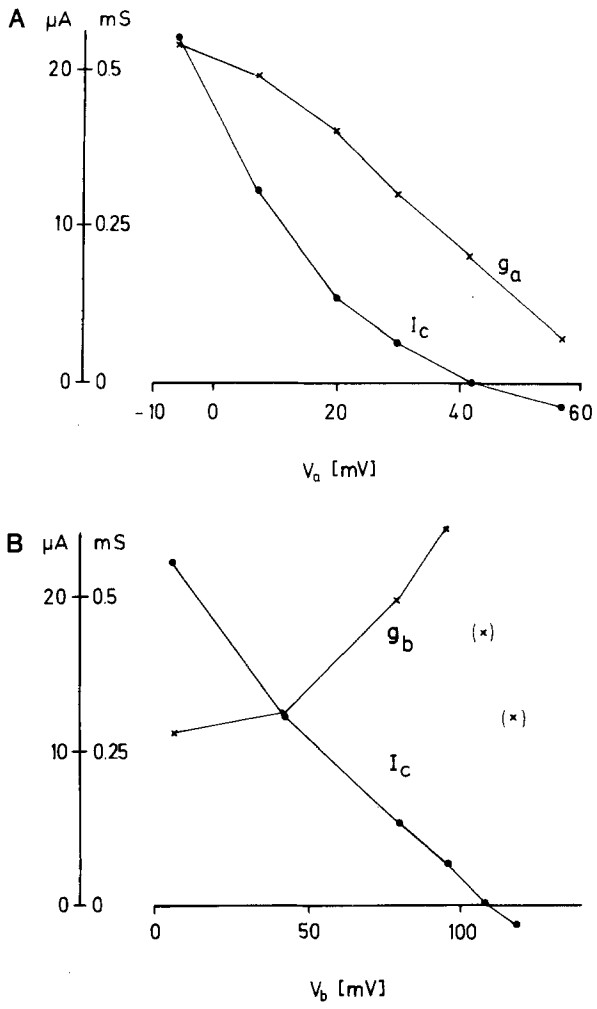

Fig. 10. (*A*) Relationship of I_c and apical conductance g_a to apical voltage V_a. (*B*) Relationship of I_c and basolateral conductance g_b to basolateral voltage V_b. This figure shows results from the experiment of Fig. 9. In (*B*) (×) indicates measurements at $V_t \geq 125$ mV, which are not meaningful (*see text*)

pathways and complete abolition of apical conductance by amiloride. The results are shown in Fig. 10, which also depicts the cellular current as a function of apical and basolateral potentials. (Note that the slopes of the current-voltage relationships are not equivalent to the g's derived by the above procedure; *see* Discussion.) As is seen, g_a declined monotonically with increasing positivity of V_a. For $V_t < 125$ mV, g_b increased with V_b, but for $V_t \geq 125$ mV, calculation of g_b becomes inexact, as explained below.

Although in most cases it was possible to calculate membrane conductances by standard means as above, occasionally interpretation was more complex. This may be seen by considering Fig. 11, showing that in several studies f_a', the voltage-divider ratio in the presence of amiloride, fell significantly below unity at high values of V_t. (Impalement artifacts were ruled out by high values of f_a' at lower values of V_t and the satisfaction of other stability criteria.) Such behavior might conceivably result either from distribution of paracellular resistance [15] or from induction of amiloride-resistant apical membrane conductance [2, 17]. Formulations permitting the calculation of membrane conductances despite these complicating factors are presented in the Appendix, Models B and C, respectively. It will be seen that as $f_a' \to 1$, the relations reduce to those of the standard model; for lower values of f_a', however, the values inferred from the three models may differ appreciably. Interestingly, values of g_a calculated according to Models B and C are identical, despite grossly different assumptions.

The relationship of g_a to apical membrane potential is shown in Fig. 12*A*. It is seen that g_a decreased uniformly with increasingly positive V_a. The calculation of g_b is more problematical, because with decrease of g_t at high values of V_t and concomitant increase of g_t' and f_a, both the numerator and denominator of Eq. (A4) become inexact. This was usually the case for $V_t \geq 125$ mV (Fig. 10*B*). The use of Eq. (B3) or Eq. (C3) cannot eliminate this problem, but permits more meaningful analysis at intermediate levels of V_t in those cases where $f_a' < 1.0$. Figure 12*B* shows the relationship between g_b and the basolateral voltage V_b for all measurements with $V_t < 125$ mV, calculated with Eq. (C3). (In this range, values of g_b calculated according to Eqs. (B3) and (C3) differed only slightly.) In general, g_b increased with V_b. Despite the limited accuracy of values of g_b, it seems clear that the complex relationship between g_c and V_t, observed with transepithelial measurements (Fig. 8), reflects the very different voltage dependencies of g_a and g_b.

Discussion

Distinguishing cellular from paracellular transport is difficult, but of evident importance for meaningful characterization of the mechanisms that regulate transepithelial transport. In earlier studies, it was often considered that the conductance of the passive (i.e., paracellular) pathway was independent of the rate of cellular transport and of the transepithelial potential, and so could be readily determined following the abolition of cell transport. While this may be the case for certain epithelia under appropriate conditions, we have found that the frog skin often manifests progressive depression of paracellular conductance after cellular transport is inhibited, whether by amiloride or by replacement of apical

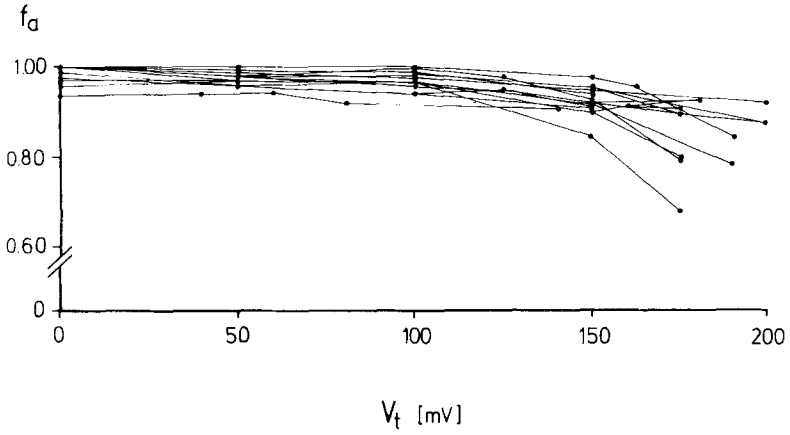

Fig. 11. Voltage (V_t) dependence of f_a', the apical voltage-divider ratio in the presence of amiloride

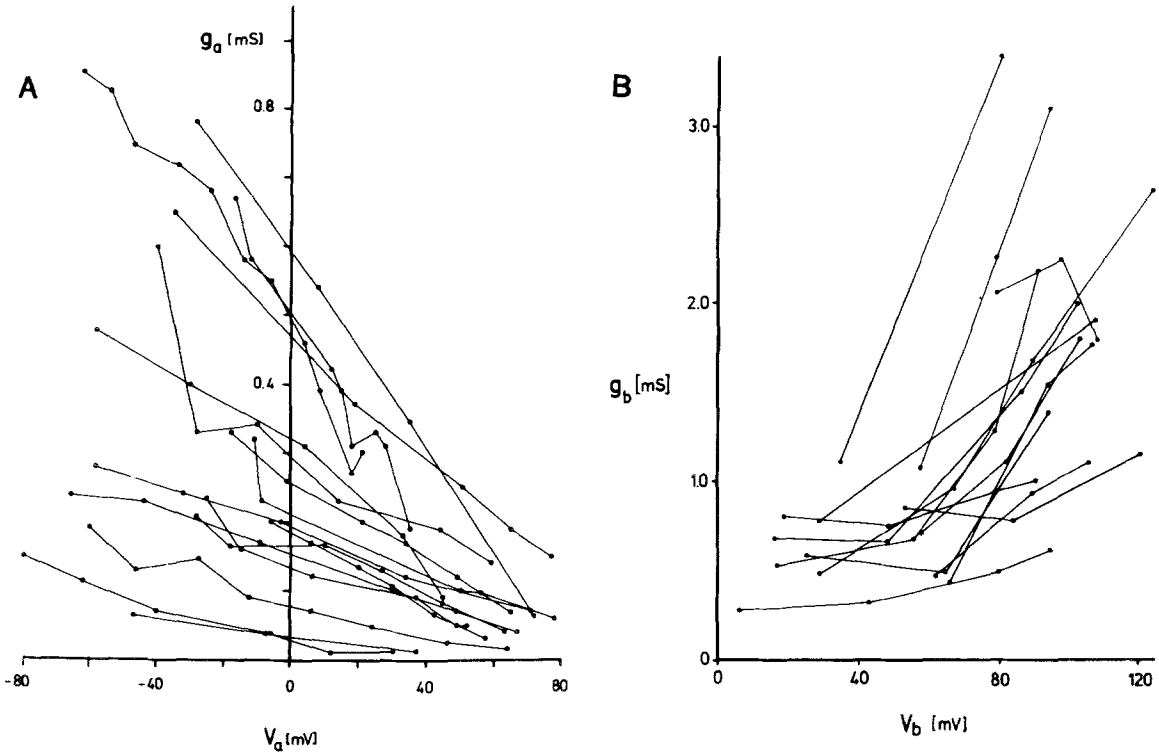

Fig. 12. (*A*) Relationship between apical conductance g_a and voltage V_a. Values of g_a were calculated with Eq. (B2) and (C2). (*B*) Relationship between basolateral conductance g_b and voltage V_b for observations in which $V_t < 125$ mV. Values of g_b were calculated with Eq. (C3); values calculated with Eq. (B3) differed only slightly

sodium (*see* Fig. 1 in ref. 14). This is especially characteristic of skins with high chloride conductance, in which it can be minimized by replacing mucosal chloride. Similar findings have been noted by Kristensen [9] and by Schoen and Erlij [18]. The latter workers report, however, that the "slow" change in conductance was seen only following the first addition of amiloride; we have seen it also after repeated applications.

Even in the absence of mucosal chloride, there remains the problem of the complex time-dependent response of the paracellular conductance to voltage, both in the absence and presence of amiloride. It was therefore apparent that the sequential technique, which necessitates exposure to amiloride for a period sufficient for the near abolition of cellular current, could not be relied upon to provide reasonable estimates of the voltage dependencies of I_c or g_c. Our transepithelial studies suggested, however, that it might be possible to cope with these complicating factors by making observations before and after very brief exposure to amiloride at each

setting of V_t, under which circumstances temporal and voltage-dependent effects are small. Microelectrode studies showed that at the reversal point, as judged by unresponsiveness of I_t to amiloride, there is also unresponsiveness of the apical voltage V_a, demonstrating constancy of apical current. This ruled out the possibility that amiloride might fortuitously depress positive cellular current and negative paracellular current to a similar extent. Accordingly, we conclude that, with appropriate caution, use of the intermittent technique permits the evaluation of cellular currents and conductances and reversal potentials more accurately than previously. Although incomplete amiloride effects result in a slight underestimate of I_c, values of conductances may be corrected for this effect (Appendix, Model C). As was mentioned, however, the intermittent technique is time consuming, and can therefore be applied only to temporally stable tissues; studies in which I_t, g_t, V_a, and f_a were not near constant at short circuit throughout the entire experimental period were discarded.

The mean value of the "reversal potential" V^r (the value of transepithelial potential at which the cell current is abolished) was 156 ± 14 mV (18 tissues, intermittent technique.) Employing the sequential technique, Goudeau et al. reported a value of V^r = 119 mV for skins of *Rana esculenta* [7]. Using the same technique, Schoen and Erlij found values of 144 and 132 mV in chloride and sulfate Ringer's, respectively, in *Rana catesbiana* [18]. Although species or protocol differences cannot be excluded, we believe that these lower estimates of V^r underestimate the actual values. In studies employing both the sequential and intermittent techniques in 12 skins, we obtained V^r's of 135 ± 32 and 164 ± 10 mV, respectively; the mean ratio was 1.31 ± 0.44. It is important to note that although setting V_t equal to V^r will abolish apical and *total* basolateral current, it cannot be assumed to abolish pump current. In fact, when basolateral (and cell) current is abolished by administration of amiloride or removal of mucosal sodium, a^c_{Na} declines progressively for several minutes, indicating continuing pump operation [6, 8].

Also of interest is the apical membrane reversal potential V^r_a, the value of V_a at which $V_t = V^r$. Before analyzing the significance of this value, it is pertinent to consider the accuracy of our measurements of membrane potentials. It is not possible, of course, completely to rule out errors, particularly because the complex protocols of the present study prevented the application of usual criteria to avoid microelectrode offset potentials. However, there is no basis for suspecting major bias; promptly after blockage of cell current with amiloride V_a averaged −103 ± 11 mV, in good agreement with the mean value of −109 ± 5 mV in an earlier study in which it was possible to apply the most rigorous criteria for the exclusion of artifacts [4].[4] At the reversal potential, the apical amiloride-sensitive current is zero. If the apical membrane were perfectly selective for sodium, the absence of amiloride-sensitive current despite a finite amiloride-sensitive conductance would demonstrate that sodium is at thermodynamic equilibrium across the apical membrane. Our previous finding of a mean cytoplasmic Na activity of 8 ± 2 mM [6] would then lead us to expect a value of V^r_a of about 60 mV, as against the mean value of 47 mV actually observed. Thus it appears that, despite the absence of apical current, there is disequilibrium, with the mean electrochemical potential of Na in the cytoplasm being lower than that in the mucosal bath. Three factors must be considered in analyzing the significance of this observation. First there is the possibility of a voltage-activated apical conductance for an ion other than Na, as found for K in the toad urinary bladder [17]. Application of the Goldman-Hodgkin-Katz zero-current relationship indicates that a P_K/P_{Na} ratio of about 0.06 could in itself account for our observations. Another possibility is that cell Na immediately adjacent to the apical plasma membrane may be higher than the average value measured with ion-selective microelectrodes and thus, at $V_a = V^r_a$, only Na near the membrane would be at equilibrium with apical Na, while a flow of sodium would persist within the cell. And finally there may also be a contribution of surface potentials. All these factors may compromise attempts to quantify a^c_{Na} from measurements of V^r_a.

With mean values of V^r and V^r_a of 154 and 47 mV, respectively, the value of V^r_b would be about 107 mV, in agreement with the values of V_b observed promptly after addition of amiloride (this paper and ref. 4). Because a^c_{Na} remains close to 8 mM within the period of 10 sec of perturbation of V_t (*unpublished observations*), the electrochemical potential difference of sodium between the cytoplasm and the serosal medium would average about 170 mV. As mentioned before, the value adequate to bring net pump sodium transport to a halt must exceed this value.

In addition to validating the intermittent tech-

[4] Amiloride was applied in concentrations of 10–50 μM and only briefly in order to improve reversibility. Because I_c remained finite at 10–15% of the control level, V_a might have been slightly more negative at full inhibition of I_c. Note, however, that incompleteness of the effect of amiloride does not affect the determination of V^r_a or V^r, which only requires absence of *change* of apical current flow.

nique, intracellular measurements permit making detailed inferences concerning apical and basolateral conductances. Certain precautions are, however, important. First, the use of brief voltage steps to measure f_a and g_t at each holding potential introduces capacitative effects, which although often insignificant at the apical surface, may distort derived values of the basolateral conductance [5, 18]. This problem can be coped with by the use of a voltage ramp [16] or, as in the present study, by lengthening the duration of the voltage pulses appropriately, usually to ≈150–400 msec. Secondly, in the standard approach commonly employed, it is assumed that the apical conductance is entirely attributable to amiloride-sensitive sodium entry, and that the cellular and paracellular pathways can be treated as discrete, so that the cell conductance g_c can be calculated as the difference of transepithelial conductance in the absence and presence of amiloride (Model A, Appendix). The apical and basolateral conductances are then calculated simply from the cell conductance g_c and the apical voltage-divider ratio. This approach is legitimate if the voltage-divider ratio f_a' in the presence of amiloride closely approximates 1.0. However, as shown in Fig. 11, this is not always the case at high V_t values. Two general mechanisms have been suggested to explain this finding. Nagel et al. [14, 15] have suggested that distribution of lateral interspace resistance can induce circulation across a highly conductive junction, and thereby lower the voltage-divider ratio significantly below unity even in tissues with low apical conductance (Model B). Mitochondria-rich cells must be considered a possible route for circulation [24, 25]. A second possible mechanism is amiloride-resistant apical conductance [2], with enhancement upon positive voltage clamping [17] (Model C).

As is shown in the Appendix, when the voltage-divider ratio f_a' in the presence of amiloride differs from unity, values of conductances calculated for either Model B or Model C differ from those of the standard formulation (Model A). Interestingly, for the apical conductance g_a, both alternative models lead to the same dependence on V_a. For g_b the voltage dependence differs for the two models in principle, but the distinction proved unimportant in the present study, because it led to significant differences only at high values of V_t, where the evaluation of $1\text{-}f_a$ became highly inexact. We have, therefore, shown the relationship of g_b to V_b only for $V_t < 125$ mV, and only for Model C. Despite the uncertainties associated with the use of our highly lumped simplified models, they facilitate understanding of the behavior of the cellular conductances. In particular, Model C compensates for the underestimation of cellular conductances associated with incomplete effects of amiloride. It is important to note the distinction between the g's calculated in the above manner, from the short voltage pulse superimposed on the holding voltage, and the slopes of the I_c-V relations shown in Fig. 10. Although the g's and the I_c-V relations are both measured at the same time, 10–30 sec after the onset of the holding voltage steps, there are discrepancies in the behavior of these two conductances. This is particularly so for the basolateral membrane, as is seen in Fig. 10*B*. Whereas g_b increased with V_b, the slope of the I_c-V_b relation initially decreased. We do not know the factors responsible for this discrepancy. The g's derived from small voltage perturbations are indicative of the membrane conductances at the particular operating point set by the holding voltage.

In an earlier study [13] in which measurements of cell conductance were unavailable, we had concluded from the voltage dependence of f_a that the depression of g_a with increase in V_a much exceeded that predicted by the constant field equation. This conclusion was based on the belief that the inner membrane conductance g_b was either constant or decreased on increase of V_b [2, 20]. The present study demonstrates, however, that in the range between short circuit and V^r, g_b *increased* with V_t and V_b. When this factor is taken into account it is found that, qualitatively, the decrease of g_a upon depolarization of the apical membrane approximates that predicted by the Goldman-Hodgkin-Katz equation. Thus our observations are not in conflict with those of others who have found the predicted I/V relationships in studies employing rapid voltage sweeps [1, 3, 18, 21, 23].

The observation of a direct relationship between g_b and V_b indicates, of course, an *inverse* relationship between g_b and I_c. This conforms with the recent finding that gradual decrease of cellular current induced by increasing concentrations of amiloride was associated with both hyperpolarization of the basolateral membrane and increase of g_b [12]. These observations differ from findings under other conditions. In studies of a tight epithelium, the *Necturus* urinary bladder, Frömter and Gebler [2] found a direct correlation between the rate of sodium transport and basolateral conductance (both parameters being evaluated from measurements in the vicinity of open circuit). Schultz et al. [21, 22], employing rapid voltage sweeps with sequential application of amiloride, inferred that basolateral conductance increased with increasing pump rate (actually increasing current, induced by varying mucosal [Na]). Lau et al. [10] found that stimulation of short-circuit current by apical sodium cotransport in a

leaky epithelium, the *Necturus* small intestine, enhanced barium-inhibitable basolateral conductance. In a subsequent study in frog skin [4], we observed a positive correlation between steady-state, short-circuit current and basolateral conductance when the spontaneous values from different untreated tissues were analyzed. On the basis of such findings, it has been suggested that with an increase of apical conductance (whether induced for example by antidiuretic hormone, aldosterone, or a rheogenic Na-coupled transport process) a parallel increase of basolateral pump function and conductance would serve both to facilitate continuing transcellular transport and to protect intracellular ionic composition [20]. Although the voltage dependence of g_b observed by us appears to contradict that assumption, it should be noted that our observations were made some 10 to 20 sec after the onset of voltage perturbation, whereas those showing positive correlations were made long after the transport rate was altered. In this regard, it is of interest to consider Schoen and Erlij's findings in the frog skin that increase in cellular current and g_a following oxytocin and insulin often precedes increase in g_b by minutes [19].

This work was supported by the Deutsche Forschungsgemeinschaft and the National Institutes of Health, Grant No. AM 29968.

References

1. DeLong, J., Civan, M.M. 1984. Apical sodium entry in split frog skin: Current-voltage relationship. *J. Membrane Biol.* **82:**25–40
2. Frömter, E., Gebler, B. 1977. Electrical properties of amphibian urinary epithelia. III. The cell membrane resistance and the effect of amiloride. *Pfluegers Arch.* **371:**99–108
3. Fuchs, W., Larsen, E.H., Lindemann, B. 1977. Current-voltage curve of sodium channels and concentration dependence of sodium permeability in frog skin. *J. Physiol. (London)* **267:**137–166
4. García-Díaz, J.F., Baxendale, L.M., Klemperer, G., Essig, A. 1985. Cell K activity in frog skin in the presence and absence of cell current. *J. Membrane Biol.* **85:**143–158
5. García-Díaz, J.F., Essig, A. 1985. Capacitative transients in voltage-clamped epithelia. *Biophys. J.* **48:**519–523
6. García-Díaz, J.F., Klemperer, G., Baxendale, L.M., Essig, A. 1986. Cell Na activity and Na pump function in frog skin. *J. Membrane Biol.* **92:**37–46
7. Goudeau, H., Wietzerbin, J., Mintz, E., Gingold, M.P., Nagel, W. 1982. Microelectrode studies of the effect of lanthanum on the electrical potential and resistance of outer and inner cell membranes of isolated frog skin. *J. Membrane Biol.* **66:**123–132
8. Harvey, B.J., Kernan, R.P. 1984. Sodium-selective microelectrode study of apical permeability in frog skin: Effects of sodium, amiloride, and ouabain. *J. Physiol. (London)* **356:**359–374
9. Kristensen, P. 1983. Exchange diffusion, electrodiffusion and rectification in the chloride transport pathway of frog skin. *J. Membrane Biol.* **72:**141–151
10. Lau, K.R., Hudson, R.L., Schultz, S.G. 1984. Cell swelling increases a barium-inhibitable potassium conductance in the basolateral membrane of *Necturus* small intestine. *Proc. Natl. Acad. Sci. USA* **81:**3591–3594
11. Nagel, W. 1976. The intracellular electrical potential profile of the frog skin epithelium. *Pfluegers Arch.* **365:**135–143
12. Nagel, W. 1985. Basolateral membrane ionic conductance in frog skin. *Pfluegers Arch.* **405 (Suppl. 1):**S39–S43
13. Nagel, W., Essig, A. 1982. Relationship of transepithelial electrical potential to membrane potentials and conductance ratios in frog skin. *J. Membrane Biol.* **69:**125–136
14. Nagel, W., García-Díaz, J.F., Essig, A. 1983. Cellular and paracellular conductance patterns in voltage-clamped frog skin. *In:* Membrane Biophysics: II. Physical Methods in the Study of Epithelia. M.A. Dinno, A.B. Callahan, and T.C. Rozell, editors. pp. 221–321. Alan R. Liss, New York
15. Nagel, W., García-Díaz, J.F., Essig, A. 1983. Contribution of junctional conductance to the cellular voltage-divider ratio in frog skins. *Pfluegers Arch.* **399:**336–341
16. Palmer, L.G. 1984. Voltage-dependent block by amiloride and other monovalent cations of apical Na channels in the toad urinary bladder. *J. Membrane Biol.* **80:**153–165
17. Palmer, L.G. 1986. Apical membrane K conductance in the toad urinary bladder. *J. Membrane Biol.* **92:**217–226
18. Schoen, H.F., Erlij, D. 1985. Current-voltage relations of the apical and basolateral membranes of the frog skin. *J. Gen. Physiol.* **86:**257–287
19. Schoen, H.F., Erlij, D. 1985. Basolateral membrane responses to transport modifiers in the frog skin epithelium. *Pfluegers Arch.* **405:**S33–S38
20. Schultz, S.G. 1981. Homocellular regulatory mechanisms in sodium-transporting epithelia: Avoidance of extinction by "flush-through". *Am. J. Physiol.* **241:**F579–F590
21. Schultz, S.G., Thompson, S.M., Hudson, R., Thomas, S.R., Suzuki, Y. 1984. Electrophysiology of *Necturus* urinary bladder: II. Time-dependent current-voltage relations of the basolateral membranes. *J. Membrane Biol.* **79:**257–269
22. Schultz, S.G., Thompson, S.M., Hudson, R., Thomas, S.R., Suzuki, Y. 1985. *Reply to:* Time dependent phenomena in voltage-clamped epithelia. *J. Membrane Biol.* **87:**175–176
23. Thompson, S.M., Suzuki, Y., Schultz, S.G. 1982. The electrophysiology of rabbit descending colon: II. Current/voltage relations of the apical membrane, the basolateral membrane, and the parallel pathways. *J. Membrane Biol.* **66:**55–61
24. Voûte, C.L., Meier, W. 1978. The mitochondria-rich cell of frog skin as hormone-sensitive "shunt-path." *J. Membrane Biol.* **(Special issue):**151–165
25. Willumsen, N., Larsen, E.H. 1985. Passive Cl currents in toad skin: Potential dependence and relation to mitochondria-rich cell density. *In:* Proc.I.Int.Congr. Comp. Physiol. Biochem. 2, Iono- and Osmoregulation. R. Gilles, editor. pp. 20–30. Springer Verlag

Received 13 June 1988

Appendix

Methods Used to Evaluate Cellular and Paracellular Parameters

The cellular pathway comprises apical and basolateral conductances in series; it is assumed that brief exposure to amiloride affects only the apical conductance.

Model A (Fig. 13A)

According to the standard analysis, transepithelial conductance is by way of discrete parallel cellular and paracellular pathways, so that for a change of the transepithelial potential, δV_t, the transcellular potential changes by $\delta V_c = \delta V_t$. The apical conductance is completely abolished by amiloride. Thus,

$$g_t = g_c + g_p$$
$$1/g_c = 1/g_a + 1/g_b$$
$$g_c/g_a = \delta V_a/\delta V_t \equiv f_a$$

and designating quantities in the presence of amiloride by a prime,

$$g_a' = g_c' = 0.$$

Accordingly, in terms of experimentally observed variables,

$$g_p = g_t' \quad \text{(A1)}$$
$$g_c = g_t - g_t' \quad \text{(A2)}$$
$$g_a = (g_t - g_t')/f_a \quad \text{(A3)}$$
$$g_b = (g_t - g_t')/(1 - f_a). \quad \text{(A4)}$$

Model B

The equivalent circuit incorporating circulation is shown in Fig. 13B. Transepithelial and transcellular voltage steps are no longer equal. Rather,

$$-\delta I = (g_c + g_j)\delta V_c = g_l(\delta V_t - \delta V_c),$$
$$\delta V_c/\delta V_t = g_l/(g_c + g_j + g_l)$$
$$g_t = -\delta I/\delta V_t \equiv (g_c + g_j)\delta V_c/\delta V_t$$
$$= (g_c + g_j)g_l/(g_c + g_j + g_l)$$

and

$$f_a = \delta V_a/\delta V_t = (\delta V_a/\delta V_c)(\delta V_c/\delta V_t)$$
$$= (g_c/g_a)[g_l/(g_c + g_j + g_l)].$$

In the presence of amiloride $g_a \equiv g_a'$ and $g_c \equiv g_c'$ become near equal as they approach zero, so that

$$g_t' = g_j g_l/(g_j + g_l)$$

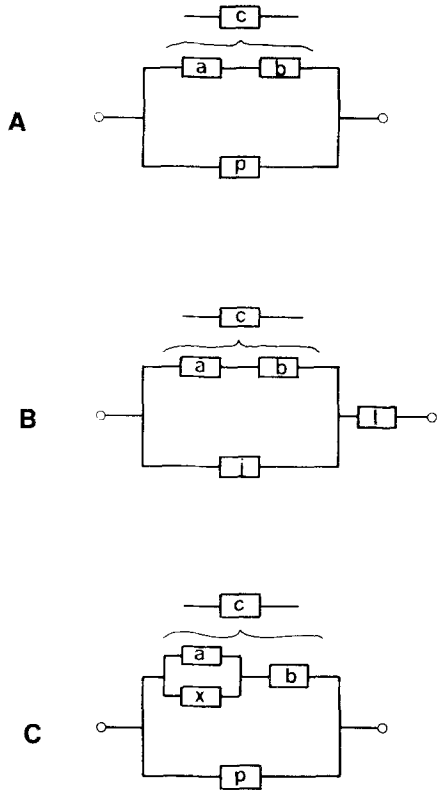

Fig. 13. Equivalent circuit models of the epithelium. (*A*) Discrete cellular (*c*) and paracellular (*p*) pathways. (*B*) Circulation model with paracellular resistance distributed between junctional (*j*) and latero-intercellular (*l*) spaces. (*C*) Apical membrane comprises an amiloride-inhibitable conductance (*a*) and an amiloride-insensitive pathway (*x*)

and

$$f_a' = g_l/(g_j + g_l).$$

Combining the relations above gives the cellular conductances

$$g_c = (g_t - g_t')\{g_t'/f_a'[g_t' - g_t(1 - f_a')]\} \quad \text{(B1)}$$
$$g_a = (g_t - g_t')/f_a f_a' \quad \text{(B2)}$$
$$g_b = (g_t - g_t')\{g_t'/f_a'[g_t'(1 - f_a) - g_t(1 - f_a')]\} \quad \text{(B3)}$$

and the paracellular conductances

$$g_j = g_t'/f_a' \quad \text{(B4)}$$

and

$$g_l = g_t'/(1 - f_a'). \quad \text{(B5)}$$

For $g_j \ll g_l$, f_a' is of the order of 1, $g_j \approx g_t' \approx g_p$, and g_l cannot be evaluated accurately.

Model C (Fig. 13*C*)

Here in parallel with the amiloride-sensitive apical conductance g_a there is an amiloride-insensitive apical conductance g_x. Therefore

$$g_t = (g_a + g_x)g_b/(g_a + g_x + g_b) + g_p$$
$$g_t' = g_x g_b/(g_x + g_b) + g_p$$
$$f_a = g_b/(g_a + g_x + g_b)$$
$$f_a' = g_b/(g_x + g_b).$$

Accordingly,

$$g_c = (g_t - g_t')\{(1 - f_a)/(f_a' - f_a)\} \quad \text{(C1)}$$
$$g_a = (g_t - g_t')/f_a f_a' \quad \text{(C2)}$$
$$g_b = (g_t - g_t')/(f_a' - f_a) \quad \text{(C3)}$$

and

$$g_x = (g_t - g_t')\{(1 - f_a')/f_a'(f_a' - f_a)\}. \quad \text{(C4)}$$